Muon spin relaxation study of phosphosilicate gels

Correspondence to:
Dr N J Clayden
School of Chemistry
University of East Anglia
Norwich
NR4 7TJ
UK

Muon Spin Relaxation Study of Phosphosilicate Gels

S Esposito, Nigel J Clayden*, and S.P. Cottrell#

Department of Applied Science and Technology,
Politecnico di Torino
Corso Duca degli Abruzzi 24, Turin 10129, Italy

*School of Chemistry
University of East Anglia
Norwich
NR4 7TJ
UK

Science and Technology Facilities Council
Rutherford Appleton Laboratory
Harwell Oxford
Didcot
OX11 0QX
UK

Abstract

Muon dynamics in phosphosilicate proton conductors P_2O_5-SiO_2 with a composition 30 mol% phosphorus oxide (30P) have been studied as a function of temperature using muon spin relaxation. For materials heat treated at 300°C the muons implant at sites close to P-OH groups associated with water molecules. While in 1000°C heat treated samples the muons are trapped at sites involving a bridging oxygen P-O-Si. Averaging of the local nuclear dipolar field by dynamics of the adsorbed water is observed above ca 180 K for the muon sites in the 300°C heat treated sample. There is some evidence for further muon dynamics in this material above 250 K perhaps caused by muon diffusion.

Keywords

Muon Dynamics proton conductor relaxation

1 Introduction

Amorphous phosphosilicate gels are of technological interest in fuel cells as part of composite electrolyte membranes [1] because of their fast proton conducting behaviour. Values for the proton conductivity as high as 10^{-1} S m^{-1} are possible [2-5] in pure materials depending on the phosphorus content and relative humidity. Moreover, the phosphosilicate gels can be readily incorporated into conducting membranes through the use of inorganic-organic composites [6,7]. The exact chemical nature of the phosphosilicate gels depends critically on the exposure of the gel to moisture while the extent of cross linking is strongly affected by the synthesis procedure and by the phosphorus content [8]. Generally, the co-polymerisation of phosphate and silicate tetrahedra takes place upon thermal treatment. However, upon exposure to atmospheric moisture the Si-O-P bonds are hydrolysed and the gels then consist of a siloxane matrix with mainly monomeric phosphorus species trapped within the pore-like structure [3,9,10]. The high proton conductivity observed in the phosphosilicate systems being attributed to the presence of adsorbed water and hydrolysed phosphate species [3]. Wideline ^{1}H NMR studies and ^{1}H spin-lattice relaxation measurements have shown that the water content of the gel, which depends on the relative humidity of the atmosphere, strongly influences the proton dynamics [11]. Similarly increasing water content also increases the proton conductivity. In particular, the similar activation energies of 10 kJmol^{-1} derived from the ^{1}H NMR and conductivity measurements at 60% relative humidity supports the idea that the dynamics seen by NMR are directly relevant to the proton conductivity. Additional evidence is provided by high resolution ^{1}H NMR studies using magic angle spinning of phosphosilicate gels with the molar compositions $10P_2O_5{\cdot}90SiO_2$ and $30P_2O_5{\cdot}70SiO_2$ which confirm the mobility of the protons as well as revealing a strong

dependence of the local hydrogen environments on the phosphorus content [12]. Thus, in the case of phosphosilicate gel with 10 mol% phosphorus oxide, a number of hydrogen environments were seen whereas in a phosphosilicate gel with higher phosphorous content only one was seen. This was attributed to fast proton exchange between the possible hydrogen sites, rather than a single unique site in the gel. Notably for both compositions the dynamics slowed significantly around 200 K, a temperature similar to the one seen for the slowing of rotational diffusive motion of H_3O^+ in $(^2H_3O)Zr_2(PO_4)_3$ and HMuO in $HZr_2(PO_4)_3 \cdot 0.16H_2O$ by ^2H NMR [13] and by muon relaxation time analysis respectively [14]. This paper describes the use of an extrinsic probe, the muon, to probe further the proton dynamics in the phosphosilicate gels. Over the past few years muon relaxation studies have proved invaluable for studying cation, principally Li^+, diffusion in battery materials through a combination of zero field and low longitudinal field measurements [15]. In these cases, the muon remains static but is sensitive to changes in the local nuclear dipolar field caused by the diffusion of the cation allowing an analysis of the muon signal in terms of a dynamic Gaussian Kubo-Toyabe hopping rate. All the materials in the current study are diamagnetic insulators thus additional low longitudinal field experiments are not required to decouple the local nuclear dipolar field and permit an electronic component to the relaxation to be determined.

Muons, in particular the positively charged muon μ^+, are potential probes for the structure and dynamics in proton conductors because μ^+ behave as a light isotope of the proton [16,17]. Thus the essential feature is that the muon, μ^+, is expected to mimic the diffusive behaviour of a proton and to a first approximation the dynamics associated with the muon will be identical to any dynamics expected for a proton in the same system. Differences in the rates of diffusion and activation energies might be

Formattato: Apice

expected based on the differing masses of a proton and the muon. In the case of the proton conducting solids studied, Nd^{3+} doped $BaCeO_3$ [16] and Sc^{3+} doped $SrZrO_3$ [17] the muon dynamics could be directly related to a proton and hence proton conductivity because there are no other sources of hydrogen dynamics. Matters are more complex in the phosphosilicate gels because of the presence of water. ~~Two~~Four ~~Three simple~~ types of dynamics can be envisaged depending on the water content, a direct ~~proton~~muon (proton~~muon~~) transfer, ~~ or~~ a water assisted muon transfer, ~~ or~~ a Grotthuss mechanism[18] or vehicle diffusion whereby the muoniated species H_2OMu^+ diffuses through the pore structure of the siloxane matrix. ~~Both~~The first three~~se~~ are shown in Figure ~~xx~~1 for a P-O-Mu grouping. ~~Only the water assisted proton transfer and Grotthuss mechanisms [ref] are is possible for an HOMu grouping.~~ The water in the Grotthuss mechanism can be $H_3O_2^+$ or a cluster such as $H_5O_2^+$ and $H_9O_4^+$ with the muoniated equivalents, for example $H_4O_2Mu^+$.

Formattato: Pedice
Formattato: Apice
Formattato: Pedice
Formattato: Apice
Formattato: Pedice
Formattato: Pedice
Formattato: Apice
Formattato: Pedice
Formattato: Pedice
Formattato: Apice
Formattato: Pedice
Formattato: Pedice
Formattato: Apice

Direct muon (proton) transfer

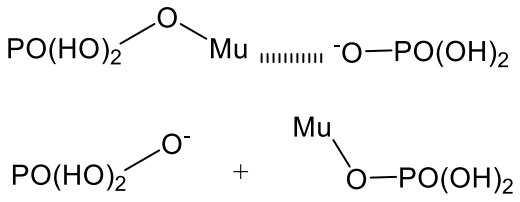

Water assisted muon (proton) transfer

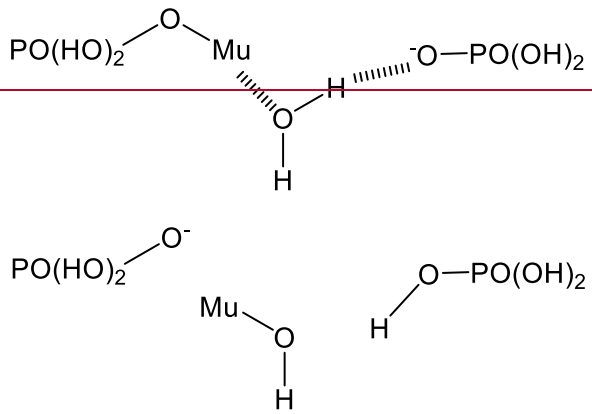

Grothuss mechanism

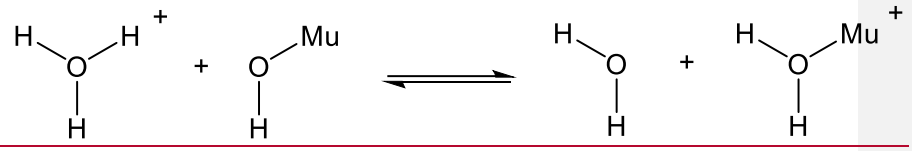

In contrast to other spectroscopic techniques, such as ^{1}H NMR where an average behaviour of protons and other hydrogens is seen when muon (μ^{+}) diffusion takes place in a muon spin experiment clearly it is the equivalent behaviour of the proton

Formattato: Apice

Formattato: Tipo di carattere: Symbol

Formattato: Apice

alone being seen. However, set against this when the trapped muon is part of a larger species, for example, $H_2O\mu^+$, the overall dynamics of this species will be monitored.. Another important feature of the muon as an extrinsic probe is that when it implants it will be trapped at sites comparable to those available to a diffusing proton, typically close to electronegative elements such as oxygen in the phosphosilicate system. Thus to understand the type of information being provided by the muon studies in the materials reported here a simple equivalence can be made between proton and muon.

Formattato: Pedice

Formattato: Tipo di carattere: Symbol

Formattato: Apice

In detail the muon relaxation rates are sensitive to the environment in which the muon comes to rest and any dynamics associated with a muon in this site. In earlier papers the muon dynamics in a crystalline proton conductor $HZr_2(PO_4)_3 \cdot{\sim}0.16H_2O$ and $Zr(H_2PO_4)(PO_4).2H_2O$ have been reported [14, 19]. Here the muon was seen to be trapped in two different diamagnetic sites. Assignment of the sites was based on the calculated second moments M_2. One, with a large M_2 was assigned to an H-O-Mu grouping and the other, with a smaller M_2, to a P-O-Mu site. Only a small amount of paramagnetic muonium appeared to be formed.

Muon trapping, given the presence of water within the gel, might thus be expected to occur at three sites: at the oxygen of a phosphate group, at a dangling Si-O and at an oxygen lone pair in any water. In the first case the species formed will be P-O-Mu which may be found either as an isolated group, or in a network formed by hydrogen bonding between water molecules and P-O-Mu. ^{31}P CP MAS NMR has provided clear evidence for the presence of significant numbers of P-O-H and hence the possibility at least, of a P-O-H network [9]. The muon signature for an isolated P-O-H is a slow decaying signal, with a relaxation rate of the order of 0.05 μs^{-1}. To the extent that an isolated Si-O mimics silica, trapping of the muon at an isolated Si-O can be expected to be dominated by a fast relaxing signal from muonium $\{\mu^+:e^{-1}\}$ and a non-relaxing

diamagnetic signal [20], although the presence of water, can be expected to introduce a relaxation the rate of which will depend on the proximity of water molecules. Initial trapping of the muon by a water molecule will lead to H_2MuO^+, however, fast proton transfer usually leads to the muon substituted molecule, HMuO [14,19]. In a proton conductor the movement of charge is likely to be facile and hence the final substituted state HMuO may well be obtained more readily, especially at lower temperatures. Regardless of the precise nature of the final state the muon signature for a muon implanted on a water molecule is a fast decaying signal with a relaxation rate of the order of 0.4 μs^{-1}. At low temperatures we can expect the muon to be immobile and show the full second moment associated with the local environment. However, with increasing temperature the local hydrogen bonded network and muon will become mobile in a manner which reflects the intrinsic proton mobility. In so doing the muon will modify its coupling to the local nuclear dipolar fields and hence its relaxation rate. Such a relaxation is most appropriately monitored in zero field and hence the emphasis on zero field muon experiments. Consequently, the muon relaxation rate observed will depend on whether water is present, the local environment of the phosphate groups and any dynamics occurring. The aim of the current work was to determine the behaviour of implanted muons in an amorphous phosphosilicate gel, P_2O_5-SiO_2 with 30 mol% P_2O_5 heat treated at 300 and 1000 °C.

2 Experimental

Phosphoryl chloride, $POCl_3$, (99%, Aldrich) and tetraethoxysilane, $Si(OC_2H_5)_4$, (99%, Gelest) (TEOS) were used as starting materials in the sol-gel preparation [21]. The 30 P_2O_5.70SiO_2 (30P) phosphosilicate gel was prepared using a procedure that has been reported in a previous paper [8]. Complete gelation occurred at room temperature in 14 days. The gelled system was held for one more day at room temperature before

drying. The gel was fully dried in air at 100 °C in an electric oven for one day. After these treatments a transparent and amorphous bulk gel was obtained. Samples subjected to two different heat treatments were studied using muon relaxation: the 30P gel heated for 30 minutes at 300ºC (30P-300) and then a further 30 minutes at 1000 ºC (30P-1000). The 30P-300 material contains intrinsic water while the 30P-1000 sample contains only a small amount of adsorbed water.

The amorphous nature of the dried gels as well as the nature of the crystallizing phases were ascertained by X-ray diffraction using a Philips diffractometer model PW1710 (CuKα) with a scan speed of 1° min [21]. While the thermal behaviour of the samples was investigated by means of thermogravimetric analysis (DSC and TGA, Thermal analyzer STA 409, Netzsch) in air, with a heating rate of 10 K min^{-1} up to 1273 K.

To determine the Brunauer–Emmett–Teller specific surface area (BET SSA) and porous volume values reported in Table 1, N_2 isotherms were measured at 77 K on samples previously outgassed at 523 K, in order to remove water and other atmospheric contaminants. The total pore volume (Vp) was determined from the amount of adsorbed N_2 at P/P0 = 0.98; both the micropore volume and external surface area were calculated according to the t-plot method. The pore size distribution (PSD) was calculated by using the non-local density functional theory (NL-DFT) method from the isotherms adsorption branches by applying a N_2-silica kernel.

Quantitative analysis of the phosphorus and silicon contents in the gel-derived glasses was performed for both gels. The two oxides were separated according to the procedure reported in ref. 22. The SiO_2 content was then determined by the gravimetric method. The phosphorus content was determined colorimetrically by

conversion to the blue phosphomolybdate complex formed by phosphorus and molybdenum in the presence of a suitable reducing agent [23].

Muons are subatomic particles with a spin I = 1/2 and it is the polarisation associated with this spin which is the property monitored in the muon experiments. Importantly muon beams generated at the ISIS muon facility, Rutherford-Appleton Laboratory, UK are close to 100% spin polarised while the polarisation of the muon at some subsequent time can be determined from the asymmetry in the muon decay. Muon having a lifetime of only 2.2 μs. Apart from transverse field (TF) experiments using a 2 mT magnetic field to determine the diamagnetic fraction, zero field was used for all the muon experiments. Zero field muon spin relaxation (ZF-μSR) measurements were made on the EMU spectrometer. In ZF-μSR no external magnetic field is applied at the time of implantation. Polarisation of the muons is determined by the asymmetry in the muon decay which is defined by Equation (1) and measured using forward (F) and backward (B) facing detectors with respect to the initial muon spin direction [24].

$$a(t) = \frac{F(t) - \alpha B(t)}{F(t) + \alpha B(t)} \qquad (1)$$

Differences in the relative efficiencies of the detectors in the forward and backward directions is accounted for by the correction factor α. Relaxation of the muon spin, as a consequence of dynamic processes, leads to a faster decay of the observed spin polarisation than would otherwise be the case simply through lifetime decay. In the absence of a magnetic field, zero field, the muon spin relaxation must occur by a spin-spin mechanism and is thus is similar to spin-spin (T_2) relaxation in NMR or ESR.

An aluminium sample holder with a circular recess 2 mm deep and 40 mm diameter was packed with the phosphosilicate gels. To prevent loss of any water in the gel an

air tight seal was then created by covering and gluing a thin Mylar film over the top of the sample and the aluminium plate. In order to study the muon dynamics the sample was first cooled to 20 K, then warmed in 20 K increments up to 300 K collecting zero field muon decays at each temperature increment. To ensure the correction factor, α, was properly known, a number of transverse field experiments were carried out at different temperatures. The derived relaxation rates were corrected for the muon lifetime. Usually 20-30 million muon decay events were collected at each field and temperature.

An in-house non-linear least squares fitting program (WiMDA version 1.306) was used for the data analysis [25] which is based on standard models for the muon implantation and decay process. Muon decays were fitted to a Kubo-Toyabe function [26] allowing the muon asymmetry and the width of the local nuclear dipolar field to be obtained. Owing to the disordered nature of phosphosilicate gels and the variety of dynamics possible, averaging of the local nuclear dipolar field was determined through the reduction in the local nuclear dipolar field in a static Kubo-Toyabe rather than using a dynamic Kubo-Toyabe with a hopping muon in a static nuclear dipolar field.

3 Results and Discussion

The analysed compositions of the 30P gel was in very good agreement with the nominal composition (Nominal $30P_2O_5 \cdot 70SiO_2$ Analyzed $27.9P_2O_5 \cdot 71.3SiO_2$) showing that the applied synthesis procedure strongly reduces the phosphorus loss in the gel-derived glasses. Therefore, the samples henceforth are labelled by their nominal compositions of P_2O_5.

Thermogravimetric analysis was employed to investigate the mass losses associated with heating the sample 30P, including losses associated with physiosorbed small molecules (water and alcohol), and with the combustion of residue organic groups. The total weight losses given by the TG curve, shown in Figure 2, was 23 wt % and it occurs below 700 K. At temperatures higher than 700 K, only a slight drift of the weight loss (about 2 wt %) occurs on the TG curves, indicating that the elimination of organic residues as well as of any volatile species is almost completed at 700 K. The loss at low temperature, about 10 wt %, is related to evaporation from open pores of water and alcohol physically trapped in the gels, while the high-temperature loss arises from burning of residual organic groups in the gels. The heat treatment of the gel (300 °C for 30 min) was chosen on the basis of the thermal analysis data; in addition, to follow the structural evolution of the gel upon heating and to force the crystallization, a further heat treatment at 1000 °C was considered.

The XRPD pattern of the 30P -300 sample exhibited a few broad reflections arising from the amorphous background indicating the precipitation of very small crystallites in the amorphous matrix [8]. As these crystals were not well formed their precise identification was not possible. Further heat treatment to 1000 °C (30P– 1000) causes the growth of the crystallites previously formed, giving rise to sharp reflections on the amorphous background. This XRD pattern gave a good match with JCPDS cards 22-1380 $Si_3(PO_4)_4$ and 40-457 $Si_5O(PO_4)_6$.

To get a greater insight into the textural properties of the gel, N_2 isotherms were measured at 77 K. The adsorption/desorption isotherm of N_2 for 30P-300 resembles the one reported by Aronne at al. for a gel with the same composition prepared in absence of alcohol and with an higher water/alkoxide molar ratio (data not reported) [10]. The shape of the isotherm is indicative of a mesoporous material with a hysteresis loop typical of materials containing pores of uniform size. The N_2 adsorption/desorption data of 30P-300 sample were determined and the corresponding textural data are reported in Table 1. Despite the small value of the BET surface area, the contribution of micropores is negligible with respect to the total pore volume confirming the mesopore nature of the 30P-300 sample.

As reported by several papers in the literature [21], the preparation of SiO_2-P_2O_5 systems is limited by the difficulty of finding a suitable phosphorus precursor that limits phosphorus losses (which can be lost as volatile monomers during heat treatments) and ensures a good degree of cross linking. Cross linking in the ^{29}Si and ^{31}P NMR spectra can be denoted by the Q_N and Q'_N notation where Q_N indicates $Si(OSi)_N(OX)_{4-N}$ and Q'_N stands for $OP(OP)_N(OX)_{3-N}$. Referring to the NMR data reported in reference 9 and shown in Figure 3 the ^{29}Si MAS NMR spectrum of 30P-300 indicates a highly cross-linked siloxane matrix involving cross-linking with phosphorus since the Q_4 resonance appears at -115 ppm. In addition, the ^{29}Si MAS NMR spectrum of 30P-300 has resonances with chemical shifts typical of six-coordinated silicon, -211 and -215 ppm [27] associated with precursors to the crystalline phases identified in the 30P-1000 C material.

The ^{31}P MAS NMR spectrum likewise indicates the presence of cross-linking through the resonances at chemical shifts more negative than -10 ppm. However, the narrow ^{31}P resonance at 0 ppm testifies to the presence of molecules of monophosphate trapped in the glassy siloxane matrix. Moreover, two resonances are also seen at -42 and -44 ppm, in Figure 3. These last two resonances are assigned to [PO_4] tetrahedra linked to [SiO_6] octahedra and [SiO_4] tetrahedral [28]. Consistent with the XRD the ^{31}P MAS NMR spectrum of 30P-1000 shows the presence of two components; one of which can be assigned to an amorphous material and the other a crystalline based on their linewidths. Crystalline phases tending to give narrower resonances because their greater order leads to a smaller chemical shift dispersion. Thus the broad resonance with spinning sidebands at -35 ppm can be assigned to an amorphous phosphoryl type material, while the sharp resonance at -44 ppm is assigned to the crystalline material. The ^{29}Si MAS NMR spectrum of 30P-1000 shows a broad resonance at -115 ppm with a narrow resonance slightly offset from the top at -120 ppm and two narrow resonances at -215 and -218 ppm, Fig. 4. As with the ^{31}P NMR spectrum the narrow resonances can be associated with a crystalline phase while the broad resonance arises from an amorphous material.

Previous experiments on $HZr_2(PO_4)_3$ [14] and $Zr(H_2PO_4)(PO_4)\cdot 2H_2O$ [19] have shown that the muon mainly implanted as a diamagnetic muon, (similar to H^+). However, in the case of the phosphosilicate gels the situation is not so clear cut. On the one hand at high temperatures the 2 mT transverse field experiments showed an asymmetry of close to 17%, compared with the maximum asymmetry of 21-23% indicating mainly a diamagnetic muon. While on the other hand at lower temperatures the diamagnetic fraction seen in the transverse field experiments for 30P-300 fell significantly to 12.6% at 20 K indicating a substantial paramagnetic fraction. No similar drop in the diamagnetic fraction occurred for the 30P-1000 samples, which gave a stable

asymmetry of around 17 % from 20 K up to 300 K. Although the phosphosilicate gels after contacting with atmospheric moisture can be considered as a silica gel type matrix with dispersed phosphorus species, there is little evidence for the muon being trapped by the siloxane which would be characterised by a muon signature with an asymmetry consisting of roughly 50% muonium, 47% non-relaxing diamagnetic and only 3% in a fast relaxing diamagnetic component [20]. The mechanism for the formation of the paramagnetic Mu is unknown, though if formed by a recombination of μ^+ with a radiolysis electron the greater fraction at low temperature would be consistent with less efficient transport of the electron away. Alternatively, the trapping site leading to the formation of the diamagnetic muon could be a thermally activated defect as has been postulated for ice [29]. A particular complication in the analysis of the muon decays seen for the phosphosilicate gels is the disordered nature of the gels resulting in the absence of well defined lattice sites to trap the muons, unlike the crystalline materials, $HZr_2(PO_4)_3$ [14] and $Zr(H_2PO_4)(PO_4)\cdot 2H_2O$ [19] studied before. Consequently a variety of different sites may well be seen which can only loosely be characterised as being associated with trapping around an acidic oxygen (a P-O-Mu) group. Similarly the local environments around a muon substituted water molecule (HMuO) may well be diverse. In both cases we can therefore expect measured parameters to be an average of any distribution. Fortunately the three types of site show sufficient differences in their local nuclear dipolar fields to allow a clear assignment. Thus the functional forms used to fit the muon decays are best seen as parameterising the signal giving an indication of the local nuclear dipolar field and hence where the muon is implanted. An estimate of the nuclear dipolar coupling can be made using:

$$\omega_d^j = \left(\frac{\mu_0}{4\pi}\right)\gamma_S\gamma_\mu\hbar r_j^{-3}$$

where γ_S and γ_μ are the magnetogyric ratios of the nuclear spin, *S* and muon, μ respectively. r_j is the distance between the nuclear spin *j* and the muon. Values of the dipolar coupling, ω_d , for P-O-Mu (r_{PMu} = 1.97 Å) and HMuO (r_{HMu} = 1.54 Å) are 0.127 x 10^6 s^{-1} and 0.609 x 10^6 s^{-1} respectively.

Both samples (30P-300 and 30P-1000) gave single component Lorentzian Kubo-Toyabe decays in the zero field muon spin relaxation (ZF-μSR) experiments, see Figure 5~~1~~, over the entire temperature range studied. While the temperature variation for both samples was described well by a Boltzmann sigmoid, Figure 6~~2~~. More typically a Gaussian form of the Kubo-Toyabe function is found in zero field μSR because the local nuclear spins are sufficiently dense to give a Gaussian distribution in the local fields. However, for the phosphosilicate materials, the nuclear spins appear to be comparatively dilute, especially in the 1000 °C heat treated sample where water has been removed leaving only residual terminal SiOH and P-OH, in which case a Lorentzian form will be more appropriate. This was evident in the muon signals themselves which have an exponential decay at short time. For a Lorentzian Kubo-Toyabe the fitting parameter *a*, is the width of the local Lorentzian field (divided by γ_μ).

At 20 K muons implanted in the 30P– 1000 material show a dipolar width of 0.032 x 10^6 s^{-1}, significantly lower than for a discrete P-O-Mu group where a value around 0.127 x 10^6 s^{-1} is expected. This implies the muon is trapped further from the phosphorus, around 3Å distant. In all likelihood this is because after heat treatment at 1000 °C almost all terminal P-OH have been lost through crosslinking either to form distinct crystalline phosphosilicate phases containing monophosphate groups fully involved in P-O-Si bonds or precursor amorphous phases with P-O-P and P-O-Si bridges. Bridging oxygens are less attractive sites to trap muons than terminal P-O

hence the muons are trapped further away. Likewise, the small dipolar coupling rules out any close association with nearby residual hydrogen from SiOH, POH or adsorbed water all of which have been shown to be present by ^{1}H NMR in the amorphous fraction [9]. Upon raising the temperature, a small decrease in the dipolar coupling is seen until between 200 and 220 K when a more marked reduction to 0.010 x 10^{6} s^{-1} takes place, after which no further changes are present up to 320 K. A transition temperature of 195.2 K is implied by the Boltzmann fit. Two explanations can be proposed for the observed temperature dependence. First, a localised hopping between different sites around the bridging oxygen and second dynamics associated with adsorbed water. Non-localised diffusion of the muon does not appear to be occurring because the local nuclear dipolar field experienced by the muon is unchanged from 240 K up to 320 K. The explanation in terms of water dynamics is less plausible since no water is present in the crystalline phases. Consequently if the temperature transition were to be attributed to water dynamics the muons would have to implant preferentially in the amorphous phase which is unlikely. Thus direct mechanisms for muon, hence proton, transfer between neighbouring acid phosphate sites whilst they can provide for a fast localised mobility of the muon to do not seem to permit fast extensive diffusion.

Turning now to the 30P – 300 sample, a much larger local nuclear dipolar field is seen for the muons at 20 K, 0.261 x 10^{6} s^{-1}, than for muons in the 30P -1000 material. This is significantly larger than predicted for a muon trapped near a phosphorus but too small for a substituted water molecule where a dipolar width of closer to 0.6 x 10^{6} s^{-1} would be expected. One plausible explanation would be the muon implants close to a terminal P–OH which is part of a hydrogen bonded network with adsorbed water. ^{31}P MAS NMR shows the presence of terminal P-OH groups [31,32]. Substitution of the hydrogen to give P-O-Mu would be suggested though by the size of the dipolar width.

Raising the temperature causes a slow reduction in the dipolar width until between 160 and 200 K when a marked reduction to only 0.033 x 10^6 s^{-1} was seen with a corresponding transition temperature of 183.9 K. Two explanations are again possible for the observed temperature variation either the muon itself is moving or the water that provides the local nuclear dipolar field through the hydrogen present in the water molecule is reorienting and or diffusing. In other water containing systems reorientation of previously rigid water molecules has been seen at around 200 K [12,13,14] suggesting this is the cause here. Reorientation of the water molecules will cause a marked reduction in the local nuclear dipolar field experienced by the muon regardless of any muon dynamics. Thus not only will the observed residual dipolar width for the muon be smaller and hence less sensitive to muon diffusion but also any muon diffusion which may be taking place will be obscured. With this interpretation the small reduction in the dipolar width below 160 K arises because of small amplitude reorientation of the water associated with the P-O-Mu species prior to isotropic reorientation rather than evidence for muon diffusion. The two mechanisms overlap to some extent because if the muon dynamics involve the muon becoming incorporated in a water cluster~~is part of a reorienting or diffusing water~~ then a reduction in the dipolar field will also occur. ~~In this case the muon results indicate no diffusion at low temperature.~~ However, the data can also be interpreted in terms of two types of muon dynamic processes with differing activation energies. One, with the lower activation energy, would be present between 20 and 150 K while the other, with the higher activation energy, that brings about the greater reduction in the muon local nuclear dipolar field would set in around 150 K. This interpretation is less plausible given the known presence of water reorientation dynamics in phosphosilicates from ^{1}H NMR spectroscopy [12]. Regardless of the exact interpretation, the data clearly shows dynamics related to proton mobility. Either the muon (proton) is diffusing or

Formattato: Apice

the water is undergoing reorientational dynamics which is crucial to the Grotthuss mechanism. Further reduction in the dipolar width takes place with increasing temperature above 200 K all the way up to 280 K giving some evidence for muon diffusion with the dipolar width becoming smaller than seen for the 30P–1000 material, 0.007 x 10^6 s^{-1} against 0.010 x 10^6 s^{-1} .

The present work demonstrates the muon implants as a diamagnetic species and is sensitive to the local nuclear dipolar field as well as changes in this caused by dynamics. Hence in principle muons could be used to study mechanisms of proton diffusion ~~,~~ However, it also shows the weakness of the method because of the manner in which the muon implanted. Thus, the principal effect seen was that associated with the reorientational dynamics of water rather than diffusive motion of the muon or proton related to the proton conductivity. By analogy with the cation diffusion in the battery systems [15], ideally the muon would implant close to a P-OH group leading to a substantial dipolar coupling with the hydrogen of this group. Then if proton conductivity led to diffusion of the acidic proton this would modulate the local nuclear dipolar field seen by the muon. Instead the muon appears to substitute at the P-OH leading to P-O-Mu or is trapped at a bridging oxygen remote from any diffusing protons. Large nuclear dipolar fields when they are seen are caused by nearby water molecules and so the muon behaviour is dominated by the dynamics of the water. The small nuclear dipolar fields remaining after dynamics removes the contribution of the water to the muon signal means the muon is not particularly sensitive to proton diffusion.

4 Conclusions

Muon dynamics in a 30 mol% P_2O_5 phosphosilicate gel, after different heat treatments, have been observed with varying temperature. The studies have established clear differences in the nature of the dynamic processes for the muon in the two materials. At low temperature two sites were seen for the trapped muon which differ in their local nuclear dipolar field. Precise identification of these sites was not possible. For 30P - 300 a site was identified as a P-O-Mu in a hydrogen bonded network with water molecules. Fast dynamics of water molecules forming part of the hydrogen bonded network was observed around 200 K in 30P- 300 leading to a significant reduction in the local nuclear dipolar field. Full averaging of this contribution to the dipolar field was complete at 220 K. Approaching room temperature a further decrease in relaxation occurred implying muon diffusion was taking place in the 30P -300 material. However, the change in dipolar width was only of the order of 0.002×10^6 s^{-1}. The second site for muon trapping seen in 30P-1000, with a smaller local nuclear dipolar width, was identified as P-O-Si :Mu, that is a muon associated with a bridging oxygen. A decrease in the relaxation rate to a smaller value occurred above 220 K owing to local muon hopping. Overall, the muons were only trapped at sites sensitive to local motion or the reorientational dynamics of intrinsic water rather than at sites sensitive to the diffusion of the muon or protons. Thus precluding a more quantitative investigation of the muon dynamics and its relationship to the proton conductivity.

Acknowledgements

We thank the Rutherford-Appleton laboratory for the use of the ISIS muon facility. We also thank Dr SJ Cox for helpful comments on the work and Dr P Baker for providing the lorentzian Kubo-Toyabe fitting routine for WiMDA.

References

[1] Xie Q, Li Y F, Chen X J, Hu J, Li L, Li H B 2015 *J. Power Sources* 282, 489-497

[2] Matsuda A, Kanzaki T, Tadanaga K, Tatsumisago M and Minami T 2002 *Solid State Ionics* 154-155 687-692

[3] Matsuda A, Kanzaki T, Tadanaga K, Tatsumisago M and Minami, T 2001 *Electrochimica Acta* 47 939-944

[4] Nogami M, Mitsuoka T, Hattori K and Daiko Y 2005 *Microporous and Mesoporous Materials* 86 349-353

[5] Li H, Dongliang J, Xiangyang K, Hengyong T, Qingchun Y and Fengjing J 2011 *Microporous and Mesoporous Materials* 138 63-67

[6] Tadanaga K, Yoshida H, Matsuda A, Minami T and Tatsumisago M 2005 *Solid State Ionics* 176 2997-2999

[7] Aparicio M, Damay F, Klein L C 2003 *J.Sol-Gel Sci. Technol.* 26 1055-1059

[8] D'Apuzzo M, Aronne A, Esposito S and Pernice, P 2000 *J.Sol-Gel Sci. Technol.* 17 247-254

[9] Clayden N J, Esposito S, Pernice P and Aronne A 2001 *J. Mater. Chem.* 11, 936-943

[10] Aronne A, Turco M, Bagnasco G, Pernice P, Di Serio M, Clayden, N J Marenna E, and Fanelli E 2005 *Chem. Mater.* 17 2081-2090

[11] Nogami M, Daiko Y, Akai T and Kasuga T 2001 *J. Phys. Chem. B* 105 4653-4656

[12] Clayden N J, Esposito S, Pernice P and Aronne A 2002 *J. Mat. Chem.* 12 3746-3753

[13] Clayden N J 1987 *Solid State Ionics* 24 117-120

[14] Clayden N J, Jayasooriya U A and Cottrell S P 2004 *Solid State Ionics* 170 51-55

[15] Mansson M, and Sugiyama J 2013 *Physica Scripta* 88 068509 - 068522

[16] Lord J S, Cottrell S P, Knight K S and Williams W G 1998 *Solid State Ionics* 115 34-345

[17] Heisel B, Hempelmann R, Hartmann O and Wappling R 2000 *Physica B* 289 487-490

~~[17]~~[18] Kreuer K D 1996 *Chem. Mater*. 8 610-641

~~[18]~~[19] Clayden N J and Cottrell S P 2006 *Phys. Chem. Chem. Phys.* 8 3094-3098

~~[19]~~[20] Arseneau D J, Fleming D G, Fyfe C A and Senba M 2003 *Physica B* 326 64-67

~~[20]~~[21] Esposito S, 2019 *Materials* 12(4), 668-693

[22] Voinovitch I A, Debras-Guedon J and Louvrier J L'analyse des silicates, Hermann, Paris, 1962, p. 467.

~~[21]~~[23] Bennet H and Hawley W G, Methods of silicate analysis, Academic Press, London, 1965, p. 130.

~~[22]~~[24] Roduner E 1988 Lecture Notes in Chemistry Springer, Heidelberg vol.49

~~[23]~~[25] Pratt, F.L. 2000 *Physica B* 289-290, 710-714

~~[24]~~[26] Kubo R and Toyabe T In: Blinc R, Hadži D, Osredkar M (eds.) 1967 *Magnetic Resonance and Relaxation*, pp. 810-823 North-Holland, Amsterdam

~~[25]~~[27] Grimmer A -R, von Lampe F and Magi M 1986 *Chem. Phys. Lett.*, 132, 549-553

~~[26]~~[28] Hartmann P, Jana C, Vogel, J, and Jager C, Chem. Phys. Letters, 1996, 258, 107-112

~~[27]~~[29] Cox S F J, Smith J A S and Symons M C R 1991 *Hyperfine Interact.* 65 993-1003

Formattato: Tipo di carattere:

Formattato: Tipo di carattere: Corsivo

[~~28~~][30] Kubo R 1981 *Hyperfine Interact*. 8 731-738

[~~29~~][31] Clayden, N J, Aronne, A, Esposito, S, and Pernice, P. 2004 *J. Non-Cryst Solids* 345-346, 601-604

[~~30~~][32] Clayden N J, Pernice P, and Aronne A 2005 *J. Non-Cryst. Solids* 351, 195-202

Table 1. Textural features of the samples as determined by adsorption/desorption isotherms of N_2 at 77 K.

Sample	**BETSSA (m^2/g)**	**Total pore volume ($cm^3\ g^{-1}$)**	**Micropores Volume ($cm^3\ g^{-1}$) [a]**	**Pore diameter (nm)[a]**
30P-300	55	0.45	1.1×10^{-3}	20-40

[a] As obtained according to the t-plot method.

[b] As obtained by applying the NL-DFT method

Figure Captions

Fig 1 Mechanisms for the transfer of a muon in a phosphosilicate gel after the muon initially implants at a site close to a phosphate group.

Fig 2 Thermogravimetric analysis of the gels containing 30% P_2O_5 (30P).

Fig 3 a) ^{29}Si and b) ^{31}P MAS NMR spectra of the gels containing 30% P2O5 (30P) at different stages of heat treatment. For ^{31}P MAS NMR spectra the resonances lying outside 5 and -50 ppm are spinning sidebands.

Fig 4 Zero field muon decay of the muons trapped at 20 K in a) 30P-300, b) 30P-1000. The solid lines represent the fit to a Lorentzian Kubo-Toyabe decay function

Fig 5 Local nuclear dipolar width as a function of temperature showing a Boltzmann fit as a solid line.

a) 30P-300, $a_{initial}$ = 0.244 MHz, a_{final} = 0.009 MHz T_{centre} = 183.9 K. χ^2/dof = 14.14

b) 30P-1000, $a_{initial}$ = 0.030 MHz, a_{final} = 0.009 MHz T_{centre} = 195.2 K. χ^2/dof = 2.36

Figure 1 generated using ChemOffice. ~~All F~~figures 4 and 5 generated using SciDAVis http://scidavis.sourceforge.net/

Figure 1.

Direct muon (proton) transfer

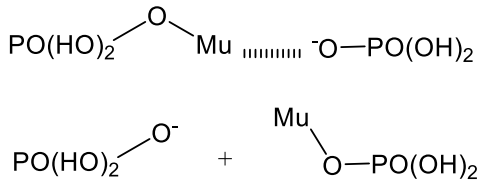

Water assisted muon (proton) transfer

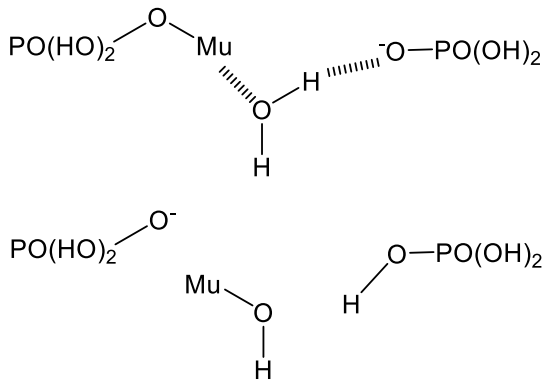

Grothuss mechanism

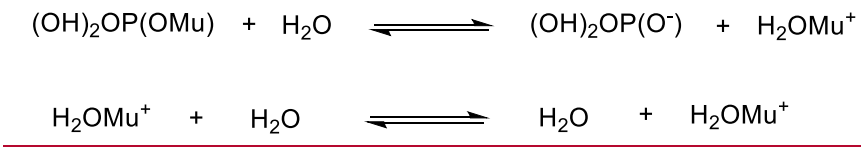

Figure 2

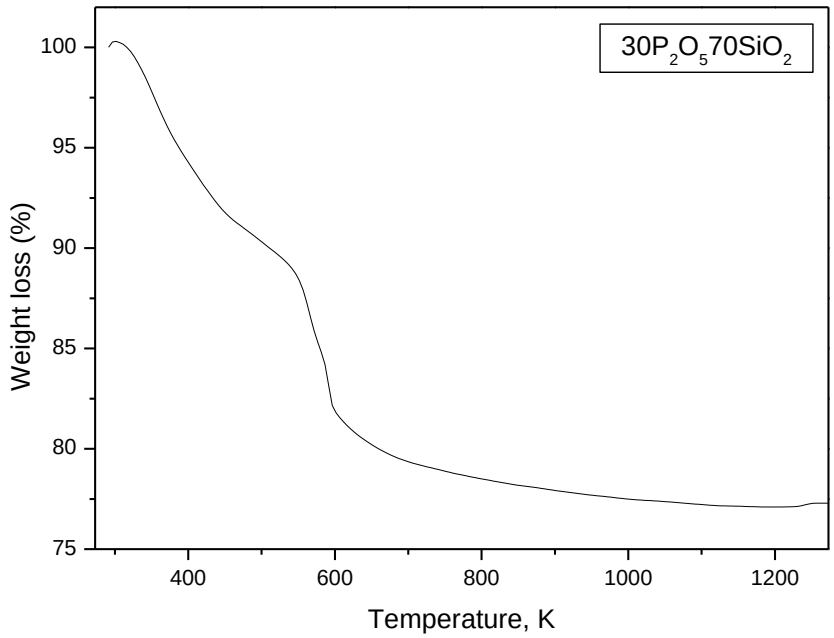
30P2O570SiO2
100
95
90
85
80
75
Weight loss (%)
400
600
800
1000
1200
Temperature, K

Figure 3

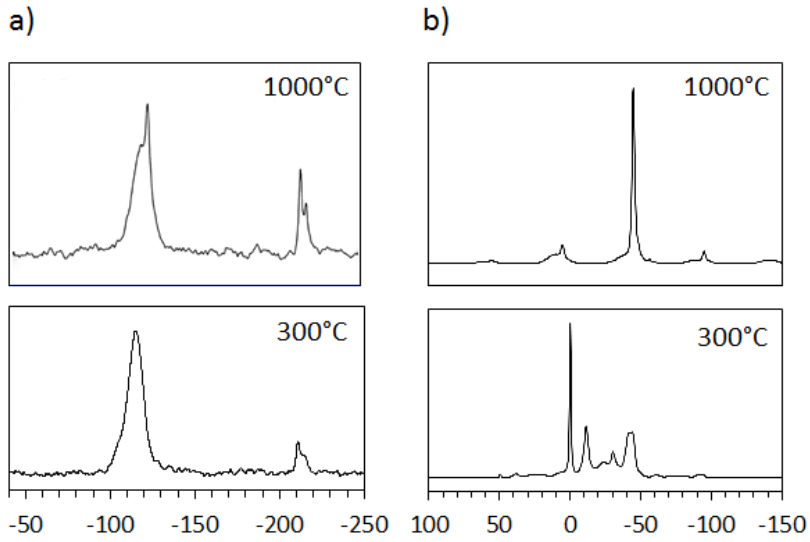

Figure 4a

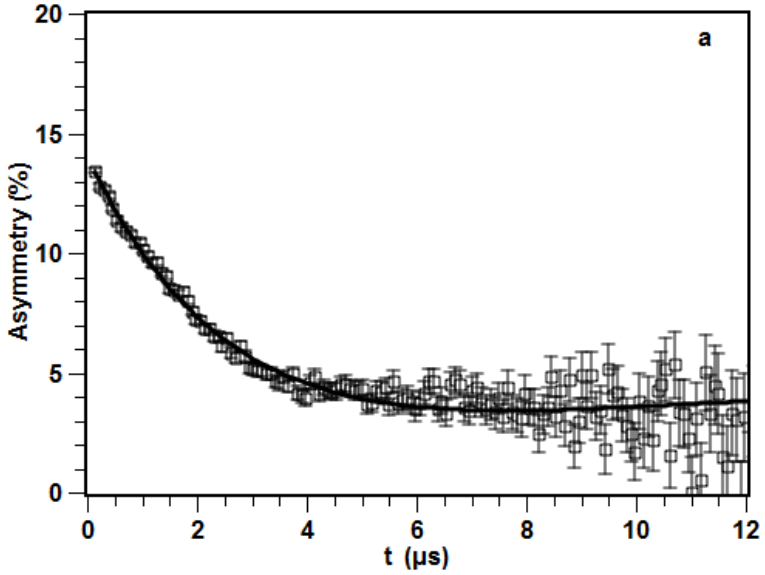

Figure 4b

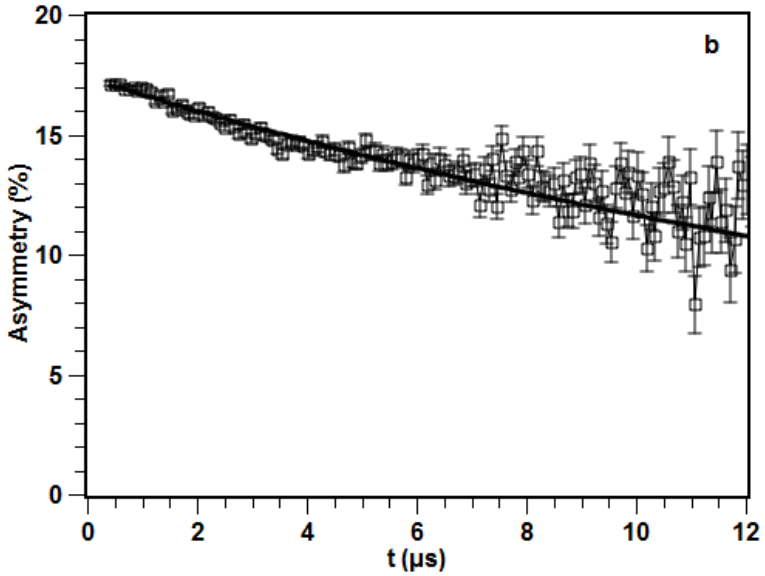

Figure 5a

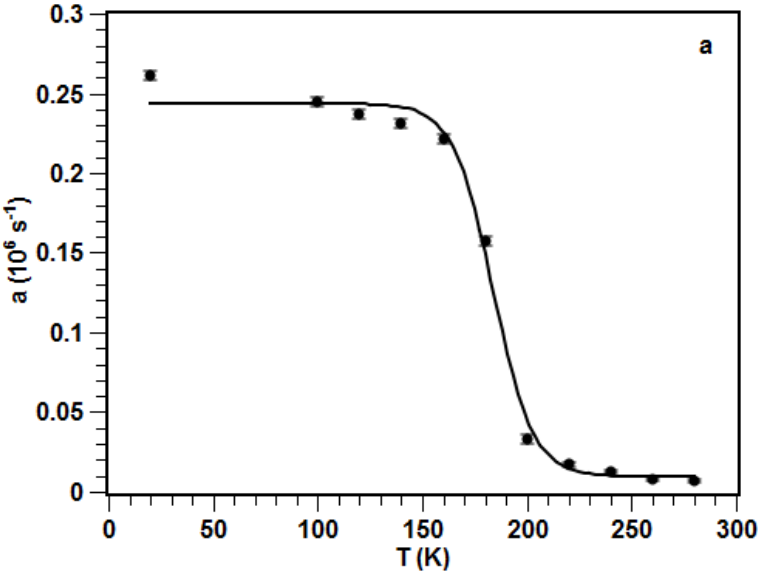

Figure 5b